Project Description – Project Proposals

Martin Brinkmann, Saarbücken

Wetting of Elastic Surface Topographies

Project Description

1 State of the art and preliminary work

1.1 State of the art

Substrate elasticity affects the shape of sessile liquid droplets if their dimensions are smaller than the elastocapillary length, being the ratio of the surface tension to the bulk elastic modulus of the wetted solid [Roman2010]. Elastocapillarity effects are particularly prominent on substrates decorated with slender surface features such as deformable posts or lamellae [Roman2010, deVolder2013]. High aspect ratio silicon structures on electronic microchips with lateral dimensions in the range of tens of nanometers may undergo irreversible damage in contact to a fluid interfaces. This “capillary collapse” is one of the main factors that limits the downscaling of the feature size in semiconductor industry [Namatsu1995] and in the fabrication of micro-mechanical devices [Raccord2004]. The balance of capillary and viscous forces during the liquid redistri-bution following an elasto-capillary instability can be utilized to control the spontaneous formation of structures through the geometry of the elastic micro-structures [deVolder2013] and the evaporation rate [Shin2018], cf. also Fig 1.

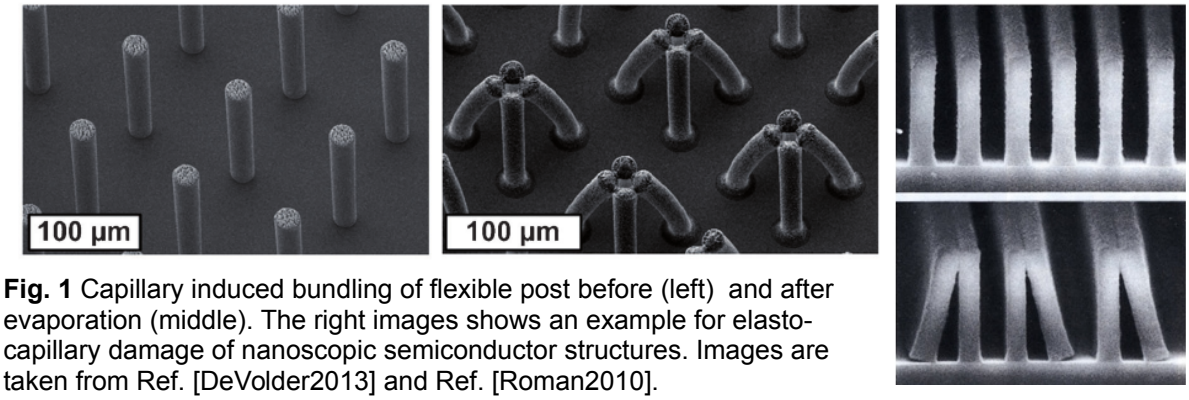

Fig. 1 Capillary induced bundling of flexible post before (left) and after evaporation (middle). The right images shows an example for elasto-capillary damage of nanoscopic semiconductor structures. Images are taken from Ref. [DeVolder2013] and Ref. [Roman2010].

It is a common experience that the elastic hair of a brush form bundles when brought into contact with a wetting liquid. The scaling of the bundle size has been derived by Bico et al. [Bico2004] considering an one dimensional array of elastic sheets that is slowly drawn out of a liquid bath. The scaling of bundle with the height above the liquid reservoir can be explained from a competition of surface energy, elastic energies and gravity. The seemingly simple problems of capillary rise between two thin elastic sheets

with clamped endpoints and held at a constant distance was solved by Kim and Mahadevan [Kim2006] which includes the shape of the sheets.

Vapor pressure controlled condensation of a perfectly wetting liquid between deformable elastic lamellae was addressed by Bernardino and Dietrich in a one-dimensional array [Bernardino2012]. It was found that the thermodynamically stable configuration of lamellae and adsorbed liquid changes from a homogeneous, undeformed state to a state with bundles comprising an increasing number of lamellae when approaching the coexistence of bulk liquid and vapor. The transitions between the homogeneous state and states with different bundle sizes are found to be always discontinuous [Bernardino2012].

To understand the basic mechanisms behind capillary collapse and bundling during evaporation, Wei and Mahadevan considered a one dimensional array of elastic lamellae during drying that is initially submerged in a wetting liquid and presented a model to describe the kinetics of the bundling process [Wei2014]. Each lamella is treated as an non-deformable plate that is anchored by a torsional spring to the bottom of the substrate. Is is assumed that, during drying, the amount of liquid in each of the compartments decreases at the same rate until the homogeneous equilibrium state becomes unstable with respect to a collective deflection of the lamellae. In a linearized theory, each of these unstable modes can be identified with an eigenvector belonging to a negative eigenvalue of the stability matrix. Based on the spectrum of unstable modes as a function of the filling degree, Wei and Mahadevan could show that the pairing, or dimer mode is always the first mode that destabilizes the initially homogeneous state during the drying process [Wei2014,Wei2015]. The bifurcation of equilibrium states underlying the instability that leads from the homogeneous state to the dimer is always supercritical and thus continuous [Wei2015]. A balance of elastic and interfacial energy can be applied to predict the maximum number of lamellae in a bundle.

In all of the above mentioned models, the volume of liquid in each compartment was treated either as fixed or as slowly decreasing with a fixed rate to account for evaporation. To the best or our knowledge, the dynamics of liquid redistribution for an intermediate case between the volume controlled and the pressure controlled case has not yet been addressed. Also works that include the dynamics of a liquid exchange between neighboring compartments driven by differences of capillary pressures appears to be missing in literature.

On rigid substrates, the stability and appearance of certain droplet morphologies in linear micro-grooves can be inferred from the interfacial free energy of a homogeneous liquid state per unit length as a function of the filling degree (i.e. the volume per unit length), the groove geometry, and Young’s contact angle [Seemann2005, Khare2007a, Khare2007b]. Equilibrium shapes of liquid confined to grooves with homogeneous cross-section can be grouped into liquid filaments which exhibit a piece-wise constant cross-section perpendicular to the direction of the grooves. The cross-section of the second class of droplet-like interfacial shapes does not exhibit a homogeneous cross-section. In contrast to the filaments the interfaces of the latter morphologies are curved also into the direction of the grooves.

A homogeneous state with a certain liquid volume per unit length is stable if the free energy per unit length is locally a convex upward function of the volume per unit length. If the upward convexity of the free energy is lost, the homogeneous state is unstable with respect to long wavelength perturbations and spontaneously segregates into a non-homogeneous state. The final state may consist of two homogeneous sections with different cross-section or a homogeneous states and state with a gradually varying cross-section [Seemann2005, Khare2007a, Khare2007b]. Here, the dry groove is considered to be one of the homogeneous state. The morphological diagram in terms of the aspect ratio of the grooves and Young's contact predicted by this effectively one dimensional model is corroborated both by experimental results and by numerical energy minimization considering the full interfacial shapes [Seemann2005]. For the sake of comparison, the local material contact angle in experiments has to be identified with Young's contact angle in numerical energy minimizations.

1.2 Preliminary work

Wetting experiments on responsive surface structures have already been carried out as part of a PhD thesis in the group of Prof. Ralf Seemann [Herrmann2015]. The experiments were focused on the bundling kinetics of two dimensional arrays of flexible lamellae in the presence of a wetting liquid during condensation and evaporation at different wetting conditions. Samples were cast from an photoresist (SU8) master in commercially available Polydimethyl-siloxane (PDMS) rubber (Sylgard 186). The typical ratio of the length of the lamellae to the periodicity of the array was 50, and thus much larger in the quasi-one dimensional samples considered by Wei and Mahadevan [Wei2014]. The aspect ratio of the lamellae reached in our experiments was $\mathrm{H/B} \simeq 6$ An oxygen plasma treatment was used to render the surface of the PDMS hydrophilic (contact angle with water $\theta \lesssim 10^\circ$). To avoid irreversible damage of the lamella arrays prior to the evaporation experiments, the samples were first submerged in an acetone bath. The acetone was then successively replaced by deionized water. To observe condensation of water from the ambient air, the samples were placed on a Peltier element for cooling. Condensation and evaporation were observed under a reflecting light microscope.

On hydrophilized PDMS samples, we could observe collapse and zipping of pairs of flexible lamellae during condensation as well as bundling of more than two lamellae during evaporation, cf. the optical images shown in Fig. 2. Time resolved recordings allowed measurements of the propagation velocities of the zippers and forming bundles into the longitudinal direction. The condensation rate was determined by placing the sample including the Peltier element for cooling on a precision laboratory scale.

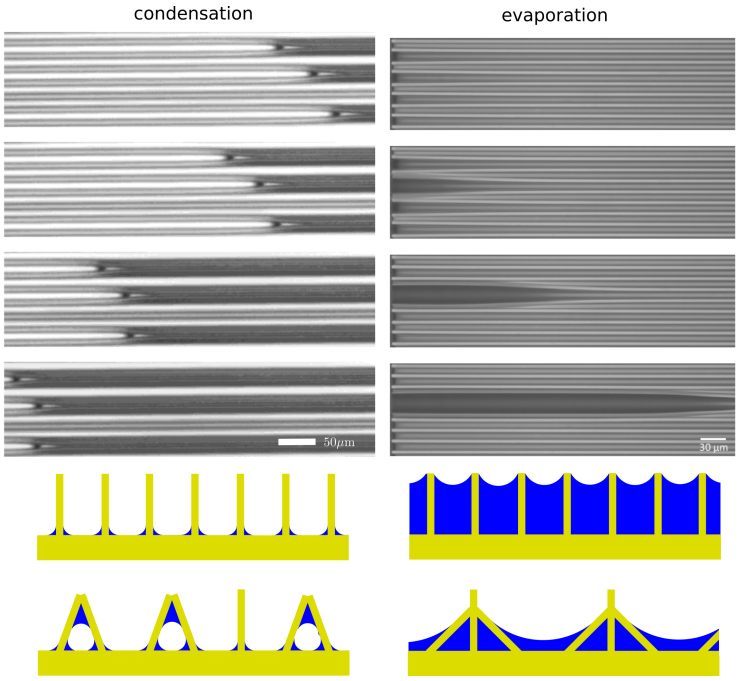

Fig.2. Left column: Time seires showing zipping of elastic lamellae made of hydrophilized PDMS observed during water condensation. Right column: Time series showing bundling during evaporation on the same substrate. The left edge of the image coincides with the left edge of the lamellae array. The time difference between each image is 9 s. Sketches of the tentative cross-sections corresponding to the emerging structures are shown in the bottom row.

But not only the condensation of water in arrays made of hydrophilized PDMS lamellae leads to spontaneous structure formation. Water droplets condensing on samples made of native hydrophobic PDMS organize themselves into a periodic pattern. This characteristically alternating droplet pattern is shown in Fig. 3(a). The different response of an elastic surface pattern during condensation on samples made of hydrophilized PDMS and samples made of native PDMS demonstrates that surface wettability is an important factor that controls the complex interplay of bulk elasticity and surface geometry during liquid condensation.

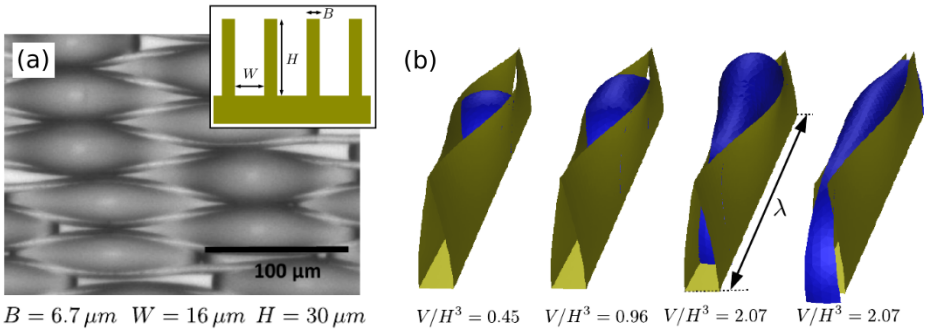

Fig. 3. (a): Droplet pattern observed during condensation of water vapor between ridges made of hydrophobic silicone rubber (Sylgard 184). (b): Numerically computed droplet shapes assuming a Young's contact angle of $\theta = (108 \pm 5)^\circ$ and for various liquid volumes rescaled by the height H of the lamella.

The spontaneous structure formation has been analyzed further using certain order parameter. A particularly simple parameter to quantify the disorder is the variance of the center to center distribution of droplets in the same groove, see the plot in Fig. 4(a). It is apparent that the rate at which the center-to-center distance $\langle d \rangle$ of the droplets increases is not monotonous with time and displays two plateaus. Between these two plateaus, the relative spread of the distance $\sigma / \langle d \rangle$ shows a flat peak, cf. also the plot in Fig. 4(a). These findings can be correlated with the increased rate of coalescences between neighboring droplets in the same groove at the end of the plateau. The cross-

talk of droplets coalesence and deformations of the lamellae are very likely the cause for the build up of long-ranged positional correlations of droplets not only in neighboring grooves. The positional correlation is best illustrated in density plot of the two point probability to find two droplets at a relative position $(\Delta X, \Delta Y)$ in Fig.4 (b) and (c).

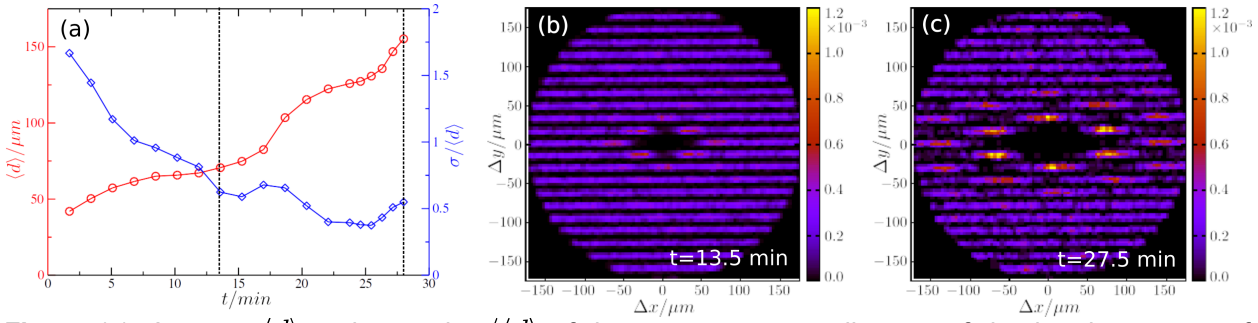

Fig. 4. (a): Average $\langle d \rangle$ and spread $\sigma / \langle d \rangle$ of the center-to-center distance of droplets in grooves of native hydrophobic PDMS. (b,c): Pair correlation function of droplet at different times as indicated by the vertical dashed lines in (a).

The final center-to-center distance is reached when the droplets cannot be anymore stay confined between the elastic lamellae. Beyond a certain maximal distance $\langle d_{max} \rangle$ the coalescence of neighboring droplets in the same groove is effectively suppressed. Numerical energy minimization of droplet shapes in contact to sinusoidally deformed lamellae shown in Fig. 3(b) reveal that the growth of the droplets into the direction of the grooves stops which prevents further coalescence. Instead, the droplets grow into the vertical direction. Large overhangs of the droplets finally lead to coalesce between droplets in neighboring grooves which leads to a quick decay of the periodic structure (not shown in Fig. 4).

Preliminary experiments with other commercially available PDMS mixtures of comparable elastic modulus (e.g. from ABCR) suggest that the ordering of the condensing water droplets depends strongly on the magnitude of contact angle hysteresis. The importance of contact angle hysteresis on the mobility and motion of droplets has been recently shown in numerical models and in wetting experiments [Semprebon2014a, Semprebon2016, deRuiter2016].

1.1 Project-related publications

[Seemann2005] R. Seemann, M. Brinkmann, E. J. Kramer, F. F. Lange, and R. Lipowsky, “Wetting morphologies at microstructured at micro-structured surfaces”, *Proc. Natl. Acad. Sci. USA* **102**: 1848-1852 (2005)

[Khare2007a] K. Khare, S. Herminghaus, J.-C. Baret, B. M. Law, M. Brinkmann, and R. Seemann, “Switching Liquid Morphologies on Linear Grooves”, *Langmuir* **23**: 12997-13006 (2007)

[Khare2007b] K. Khare, M. Brinkmann, B. M. Law, E. L. Gurevich, S. Herminghaus, and R. Seemann, “Dewetting of Liquid Filaments in Wedge-Shaped Grooves”, *Langmuir* **23**: 12138-12141 (2007)

[Semprebon2012] C. Semprebon, S. Herminghaus, and M. Brinkmann “Advancing modes on regularly patterned substrates”, *Soft Matter* **8**: 6301 (2012)

[Semprebon2014a] C. Semprebon and M. Brinkmann, “On the onset of drop motion”, *Soft Matter* **10**: 3325-3334 (2014)

[Semprebon2014b] C. Semprebon, P. Forsberg, C. Priest, and M. Brinkmann, “Pinning and wicking in regular pillar arrays”, *Soft Matter* **10**, 5739 (2014)

[Semprebon2016] C. Semprebon, S. Varagnolo, D. Filippi, L. Perlini, M. Pierno, and M. Brinkmann, and G. Mistura", "Deviation of sliding drops at a chemical step", *Soft Matter* **12**: 8268-8273 (2016)

[deRuiter2016] R. de Ruiter, C. Semprebon, M. van Gorcum, M. H. G. Duits, M Brinkmann, and F. Mugele, “Stability limits of capillary bridges: how contact angle hysteresis affects morphology transitions of liquid microstructures”, *Phys. Rev. Lett.* **114**: 234501 (2015)

[Semprebon2018] C. Semprebon, C. Herrmann, B-Y Liu, R. Seemann, and M. Brinkmann, “Shape Evolution of Droplets Growing on Linear Microgrooves”, *Langmuir* **11***:* 10498-10511 (2018)

1.1.1 Articles published by outlets with scientific quality assurance, book publications, and works accepted for publication but not yet published.

n.a.

1.1.2 Other publications

n.a.

1.1.3 Patents

1.1.3.1 Pending

n.a.

1.1.3.2 Issued

n.a.

2 Objectives and work programme

2.1 Anticipated total duration of the project

Three years

2.2 Objectives

The proposed project aims to understand the kinetics of certain elasto-capillary instabilities from an interplay between the deformations of the surface features, the elasticity of the substrate material, and the transport of liquid in wetting films during condensation or evaporation. In particular, we will extend the effectively one-dimensional models for condensation and evaporation of a perfectly wetting liquid to

two-dimensional periodic arrays of linear lamellae in contact to partially wetting liquids, i.e. with an liquid air interface that form a finite contact angle on the substrate. One of the central goals is to identify the physical quantities and factors that control the velocities of the zipping instability observed during condensation and the bundling kinetics during evaporation. To this end, we intend to perform systematic condensation experiments for various geometries of the lamella arrays. This is complemented by modeling the instability using a long-wavelength approximation for the transport of the liquid. The long-wavelength model for liquid transport and deformation must allow for contributions to the elastic energy arising from bending deformations into the direction of the lamellae to account for variations of the lamellae contour and liquid volume in longitudinal direction. As contact angle hysteresis controls the coalescence and mutual displacement of water droplets that are growing in the gap between two neighboring lamellae, the long-wavelength model must also account for a difference between static advancing and static receding contact angles.

A central goal of the projects to develop an adequate description of the mechanical equilibrium and the dynamics from the functionals of the interfacial and elastic energies functionals. These energy functionals shall include the coupling between local deformations of the walls in vertical and longitudinal direction and the distribution of the liquid into the direction of the lamellae. Both functionals are complemented with an additional dissipation functional that accounts for viscous flows and, potentially, also for dissipation related to contact line motion and static contact angle hysteresis. This general formulation shall serve us as a starting point to derive a set of coupled evolution equations for the displacement of the ridges and the local filling degree on the basis on the variational principal of least dissipation [Doi2011].

In addition to the responsive surfaces with elastic surface features we will model wetting of a periodic two-dimensional array of micro posts of a elastically deformable materials. In contrast to the aspect ratio of the posts, it is possible to change the distance and relative orientation of the posts by stretching or bending of the base surface. Previous numerical studies [Semprebon2012, Semprebon2014b] have evidenced a range of material contact angles where the formation of a wicking liquid film as well as the apparent advancing and receding contact angle of a macroscopic liquid droplet depend sensitively on the post density. In this range of control parameters, we expect to find a strong dependence of the wetting and wicking behavior of the liquid on the elasticity of the material.

2.3 Work programme incl. proposed research methods

To achieve the goals as outlined in section 2.2, we will plan to implement the following work packages (WP):

WP 1: Condensation in regular arrays of hydrophilic lamellae

This work package aims at a continuation of the condensation experiments presented in section 1.2. To identify the mechanisms that control the velocity of the zipping instability,

we intend to conduct condensation experiments for different geometries of linear surface patterns. We plan to prepare samples with various lamella arrays each for a different combinations of height to thickness ratios as well as the height to distance ratio. To avoid the use of a humidity controlled housing for the entire experimental set-up, we plan to record water condensation and subsequent zipping simultaneously on multiple arrays that are placed on the same Peltier element. This ensures that each lamella array experiences the same cooling rate and relative humidity. Following the preliminary work outlined in Ref. [Herrmann2015], the condensation rate will be determined from the mass of adsorbed water measured with a laboratory scale. Water condensation and zipper motion will be monitored with a CMOS camera (PCO) that is mounted on a reflecting light microscope (Zeiss Axiophot).

Nucleation of the collapsed regions occurs mostly on at the edge of the lamella arrays. On some samples the nucleation occurs also in the central part of an array. To further investigate the mechanisms that control the nucleation and the further propagation of the collapsed segments, we intend to fabricate samples with heterogeneous lamellae. A starting point for these experiments are samples with lamellae whose thickness increases in steps. Here, one can expect that the collapsed parts of the lamellae are arrested at these discontinuities and continue to move only if a certain volume per unit length in the non-collapsed region has been reached.

WP 2: Long wave length approximation for lamella deflection and liquid transport

The effectively one-dimensional model that considers the free energy as a function of the local filling degree serves as a starting point to model the evolution of liquid morphologies during condensation in an periodic array of elastically deformable lamellae. Starting point of the model is an energy functional of the form:

$$\mathcal{F}_{int}\{v\} = \int \mathrm{d}x \, \left[g\left(v(x)\right) \left(\partial_x v(x)\right)^2 + f\left(v(x)\right) \right] \tag{1}$$

which describes the interfacial free energy of a liquid filament with a filling degree that varies along the direction of the grooves. The particular form of the functions $\mathrm{g(v)}$ and $\mathrm{f(v)}$ depend on the aspect ratio $\mathrm{H/W}$ and Young's contact angle θ_0. Assuming the contour of the interface in a vertical cross section to be a circular arc, one can derive the from of the functions $\mathrm{f(v)}$ and of the prefactor $\mathrm{g(v)}$ employing the calculus of differential geometry [Seemann2005, Khare2007a, Ruiz-Guiterrez2018].

Deformations of the lamellae cause a heterogeneous distribution of liquid and can be included to the model by vritue of a dependence of $\mathrm{f(v)}$ and $\mathrm{g(v)}$ on the varying cross-section of the groove. To reach an analytically and numerically tractable model, a number of simplifications are in order. In particular, the curvature of the lamella contour in vertical direction will not be resolved in the model [Bernardino2012, Wei2014, Wei2015]. Deformations of the walls are simply taken into account by a tilt angle ϕ_i at the base of lamella i. In this context, Wei et al. proposed to resort to Timoshenko beam theory for an estimate of the related torsional spring constant if the aspect ratio of the lamellae is small [Wei2015]. Also the fact that the substrate is made of the same elastic material as the lamellae gives rise to a "hinge effect" that needs to be taken into account [Wei2015].

The relation between the local filling degree $\mathrm{v(x)}$ and the free energy per unit length, of the groove between the two adjacent lamellae i and $\mathrm{i{+}1}$, $\mathrm{f}(\phi_i, \phi_{i+1}, v)$, is also taken to depend on the difference $\Delta\phi_i = \phi_{i+1} - \phi_i$ of the tilting angles of the two adjacent walls. A small simultaneous tilt of the two adjacent walls into the same direction, i.e. deformations that keep the distance of two neighboring ridges constant will change the free energy function only in a quadratic order and will thus be neglected. The corresponding free energy function $\mathrm{f}(\Delta\phi, v)$ that accounts for the tilt has been derived from simple geometrical considerations in, e.g., the work of Wei et al. Ref.[Wei2015]. In full analogy to the case of linear grooves with a constant cross section, it is straight forward to compute the corresponding prefactor $\mathrm{g}(\Delta\phi, v)$ in front of the squared gradient terms from a simple approximative parameterization of the free interface by by circular arcs [Ruiz-Guiterrez2018].

Equilibrium shapes are stationary points of the energy functional under the constraint of a globally conserved volume. Hence, the shape of an interface in mechanical equilibrium satisfies a corresponding Euler-Lagrange equation which is tantamount to relation between the local pressure in the liquid and the local mean curvature of the free interface [Seemann2005, Khare2007a, Khare2007b]. This observation can be used to construct positive definite quadratic form that serve as an energy functional from a certain class of shape equation.

Elastic energy: The work required to deform the grooves must be included to the free energy functional if the liquid interface is strong enough to deform the lamellae. Deflections of the ridges are captured in the simple model proposed by Wei and Mahadevan [Wei2014]. The walls as rigid plates of unit depth elastically hinged at the base. Assuming ridges with a straight cross-section implies a substantial simplification of the interfacial free energy per unit length. The main contribution to the elastic energy will be the spring energy $\mathrm{F}_{sp} = k_{sp}\phi^2$ related to the local deflection angle $\phi(x)$. The torsional spring with a spring constant k_{sp} at the hinge. An additional energy term $\mathrm{F}_{bend} = k_{bend}(\partial^2_{xx}\phi)^2$ accounts for the effective bending stiffness of the flexible lamellae. Elastic energy stored in stretching can be included by a fourth order term $\mathrm{F}_{st} = k_{st}(\partial_x\phi)^4$ in the first derivative of the deflection angle, and may be neglected in a first approach. The magnitude of the effective bending rigidity k_{bend} of the lamellae can be estimated from the elastic energy under a harmonically varying lateral force acting on the top ridge.

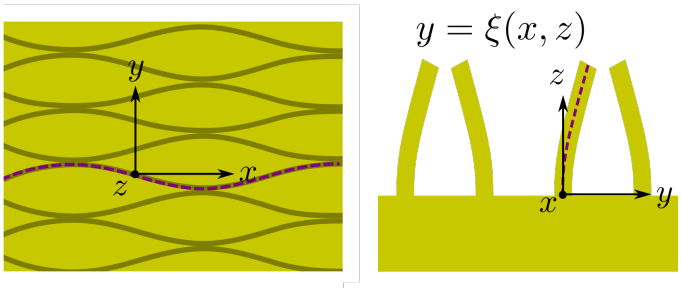

Fig.5 Sketch of the deformed lamellae indicating the horizontal deflection in top view (left) an in side view (right). The deflection is parameterized in a Monge representation of the form $\mathrm{y}{=}\xi(x, u)$.

According to the thin plate theory for small displacements $\xi(x,z)$ satisfies:

$$(\partial_{xx}^2+\partial_{zz}^2)^2\xi(x,z)=0 \qquad \text{on} \qquad (x,z)\in\mathbb{R}\times[0,H]$$

with boundary clamped conditions at the bottom:

$$\xi(x,0)=0 \quad \text{an} \quad (\partial_z\xi)(x,0)=0 \qquad \text{for} \qquad x\in\mathbb{R}$$

and a prescribed deflection at the top edge without a bending moment parallel to the edge:

$$\xi(x,H)=a\sin(kx) \ \text{ and } \ (\partial_{xx}+\nu\partial_{zz})\xi(x,H)=0 \quad \text{for} \quad x\in\mathbb{R}$$

The total elastic energy per unit length can be obtained from the solution $\xi(x,z)$ through the integral:

$$\mathcal{E}_{el}=\kappa\tfrac{k}{2\pi}\int_0^{2\pi/k}\mathrm{d}x\int_0^H\mathrm{d}z\left[(\partial_{xx}^2+\partial_{zz}^2)\xi(x,z)\right]^2$$

where $\kappa=EB^3/12(1-\nu)$ is the bending rigidity of a thin plate of thickness B, elastic modulus E and Poisson ratio ν. The effective bending rigidity of the lamellae can be identified from the fourth order coefficient in an expansion of $\mathcal{E}_{el}$ in powers of the wave number k.

Liquid mobility: Complemented with a corresponding dissipation functional the energy functional (1), can be employed to derive a consistent gradient dynamics that describes the temporal evolution of the local filling degreee and the deflection angle of the lamellae. In the considered one-dimensional representation of the liquid state, this dissipation functional is based on the approximation of a locally homogeneous cross-section of the liquid. The prefactor of the quadratic dissipation functional can be identified with the mobility of a viscous liquid in the Stokes limit, i.e. given by the volume flux divided by the pressure gradient. For a given shape of the walls and interface one can easily compute the mobility from the solution to a two-dimensional Poisson equation for the longitudinal component of the flow velocity with appropriate no-slip and zero traction boundary conditions by applying finite element methods (FEM) or boundary element methods (BEM). In full analogy to the functions $\mathrm{f}(\Delta\phi,v)$ and $\mathrm{g}(\Delta\phi,v)$ in the energy functional (5), we suppose that the prefactor of the corresponding quadratic form of the dissipation functional depends only on the difference of tilt angles, $\Delta\phi$.

WP 3: Modeling the zipping dynamics

Experimental results obtained in WP 2 shall be compared with predictions obtained in a fluid dynamic model based on a long-wavelength approximation. The coupled set of one-dimensional evolution equations describing the lamella deflections and the volume per unit length as a function of time shall be derived from a approximative expression for the interfacial free energy and liquid mobility. The details of this model are outlined in

the previous work package WP2. In accordance with the condensation experiments, we will consider a perfectly wetting Newtonian liquid like pure water.

According to the investigations of Bernardino and Dietrich which were restricted to homogeneous states of the lamellae and liquid [Bernardino2015], the transition between two non-coalesced menisci and a single meniscus spanning between two bend lamellae in the capillary pressure controlled ensemble is discontinuous. From this observation we expect not only a non-zero driving force per unit length acting on the zipping front but also a finite difference of the capillary pressure in the liquid of the shrinking segment with two separate menisci and the growing segment where the two lamellae have closed up, c.f. also the images shown in Fig. 2. By construction, the long wavelength approximation for liquid transport and deformation considers only flows into the longitudinal direction along the lamellae and discards any viscous dissipation related to flows into the spanwise direction. The present work package can help to answer the question whether the latter flow mode has an influence on the zipping dynamics.

This work package shall also answer the question of how the rate of condensation affects the zipping velocity of the meniscus. The kinetics of water condensation from the ambient air can be modeled through a source terms that is proportional to the local surface area, i.e. the arc length of the free liquid interface contour in a cross-section. Hence, the closing up of the two lamellae while zipping should have a profound effect on the total mass flux into the non-collapsed segment where the liquid wets the interior edge formed by the bottom of the substrate and the lamellae. If the adsorption rate is the dominant factor that controls the velocity of the zipping front, one must observe a slowing down of the zipping front as the fraction of collapsed lamellae segment in a row increases. If, one the contrary, the zipping velocity is controlled by the redistribution of water between the non-collapsed segments and the segments of collapsed lamellae, the zipping velocity must be insensitive to the condensation rate.

WP 4: Evaporation from a regular array of hydrophilic lamella

Aim of this work package is to identify the factors that control the onset of the bundling instability in a periodic array of elastically deformable lamellea. The images presented in the preliminary work section Fig.2 indicate that the onset of the bundling instability occurs always at the side of the array. Initially, the instability appears to drive the system towards a state consisting of dimers of neighboring lamellae. But in the course of the evaporation the dimer mode decays. Simultaneously a higher order pairing mode leading to three or four lamellae in a single bundle finally prevails. To understand the role of the liquid redistribution on the particular pathway, we intend to perform evaporation experiments with liquids of different dynamic viscosities. The results of preliminary evaporation experiments reported in Ref. [Herrmann2015], employing aqueous solutions of dextrane with different dynamic viscosity but identical evaporation rate, show a clear dependence of the velocity of the propagating fronts. Similar to the tasks in work package WP 1, we intend to record the bundling on samples of varying geometry, including different ratios H/B of lamella height H to thickeness B, and different aspect ratios H/W of lamella height to spacing W.

The second task of the work package is to adapt the long-wavelength model developed in WP 2 to the situation encountered during evaporation of water from periodic array of hydrophilic lamellae. Here, we will investigate the role of longitudinal liquid transport on the kinetics of the progressing instability. Led by the observation that the bundling instability always starts from one end of the lamella array, we will place a special focus on the boundary conditions for the coupled evolution equations of local tilt angle and filling degree. Here we expect that certain modifications of the evolution equations are required to account for the particular boundary effects on the elastic energy. Numerical energy minimization will be employed to estimate additional contributions to the interfacial energy which reflect the excess of free interface at the terminal parts of the lamella rows.

WP 5: Condensation in arrays of partially wettable lamellae

This work package is dedicated to the experimental investigation of the condensation and coalescence dynamics of water droplets for the case of high contact angles. Following the idea to explore the influence of the magnitude of contact angle hysteresis on a native PDMS surface, we will repeat the condensation experiments with samples made of different types of PDMS. Here, we intend to examine the correlation of the degree of pattern formation and the mobility of water droplets during condensation. If possible also the elastic modulus shall be varied to quantify the impact of the bulk elasticity on the condensation pattern for samples with identical substrate geometry.

Besides the standard soft photolithography approach, we intend to use samples produced with alternative fabrication methods obtaine in the group of Prof. Leonid Ionov at the University of Bayreuth within the proposed project in the present SPP. These fabrication methods can be applied to a large variety of surface topographies and polymeric materials with different wetting properties. This open the possibility for a systematic study of intermediate case between the condensation on strongly hydrophilic elastic substrates as proposed in WP 1, and moderate hydrophobic materials like PDMS in the present work package.

The coalescene dynamics and interaction of partially wetting droplets in contact to soft substrates is also addressed in the joint project of Prof. Snoeijer form the University Twente and Prof. Uwe Thiele from the University of Münster. This project is focused on the interaction of droplets mediated by elastic deformation of a plane substrate. The present project may greatly benefit from shared results and experiences in modeling of these systems obtained withing the framework of the SPP.

WP 6: Long-wavelength model with contact angle hysteresis

This work package aims at an extension of the formalism to account for contact angle hysteresis in the coarse grained model. This will be necessary to describe the motion and coalescence dynamics of droplets on the native PDMS during condensation. To this end, we need to add further terms in the dissipation functional that will modify the coupled set of one-dimensional equations developed in WP 2 in the presence of static contact angle hysteresis. A distinction between advancing and receding contact angles

will be particularly important for the case of partially wetting fluids where the interfacial free energy per unit length forms distinct branches for each of the homogeneous states with a different meniscus topoglogy. The implementation of static contact angle hysteresis within a variational framework and the derivation of consistent equations to describe the evolution of the liquid are addressed in the project proposed by Dr. Dirk Peschka at the WIAS Berlin. The coarse grained model for liquid transport and deformation in the present project are ideal instances to apply the variational approach to derive a consistent set of evolution equations.

WP 7: Wicking into arrays of flexible posts

The final work package addresses the role of substrate elasticity for the conditions and kinetics of spontaneous film spreading in regular periodic arrays of posts with circular and square cross section. Previous investigation revealed that the conditions for wetting and film spreading depend sensitively on the advancing material contact angle [Semprebon2012, Semprebon2014b]. So far, the mechanisms controlling interface and spontaneous film formation have been evaluated only for post arrays made of rigid materials. Using the fabrication methods available in the group of Prof. Leonid Ionov from the University of Bayreuth opens the possibility to prepare samples of elastic materials that are sufficiently soft to observe the bending of posts in the presence of capillary stresses. The structural feed back potentially leads to a modification of the conditions for spontaneous wicking into the post array in terms of the material contact angle.

2.4 Data handling

All data obtained in experiments and in numerical investigations will be stored and secured on a fileserver in the IT service of the Saaland Universtiy. Backups of publication relevant data will addionally kept for 10 years on external hard drives.

2.5 Other information

2.6 Descriptions of proposed investigations involving experiments on humans, human materials or animals as well as dual use research of concern

n.a.

2.7 Information on scientific and financial involvement of international cooperation partners

n.a.

3 Bibliography

[Bico2004] R. Bico, B. Roman, and A. Boudaoud, “Adhesion: elastocapillary coalescence in wet hair.“ *Nature* **9***:* 690 (2004)

[Ciarletta2017] P. Ciarletta, D. Vella, „Patterning through instabilities in complex media: theory and applications“, *Phil. Trans. R. Soc. A* **375**: 20160442 (2017)

[Chandra2009] D. Chandra and S. Yang, “Capillary-Force-Induced Clustering of Micro-pillar Arrays: Is It Caused by Isolated Capillary Bridges or by the Lateral Capillary Meniscus Interaction Force?”, *Langmuir* **25**: 10430-10434 (2009)

[DeVolder2013] M. De Volder and A. J. Hart, “Engineering Hierarchical Nanostructures by Elastocapillary Self-Assembly”, *Angew. Chem. Int. Ed.* **52**: 2412-2425 (2013)

[Doi2011] M. Doi, “Onsager’s variational principle in soft matter”, *J. Phys.: Condens. Matter* **23** 284118 (2011)

[Hadjitofis2016] A. Hadjittofis, J.R. Lister, K. Singh, and D. Vella, “Evaporation effects in elastocapillary aggregation“, *J. Fluid Mech.* **792**: 168-185 (2016)

[Herrmann2015] Carsten Herrmann (2015), “Experimentelle Untersuchungen zum Benetzungsverhalten fester und elastischer linearer Grabenstrukturen“, PhD thesis (in German), Saarland University. doi:10.22028/D291-23127

[Kim2006] H.-Y. Kim and L. Mahadevan, “Capillary rise between elastic sheets“, *J. Fluid Mech.* **548**:141-150 (2006)

[Ledesma-Aguilar2017] R. Ledesma-Aguilar, G. Laghezza, J. M Yeomans, and D. Vella, “Using evaporation to control capillary instabilities in micro-systems“, *Soft Matter* **13**: 8947-8956 (2017)

[Namatsu1995] H. Namatsu, K. Kurihara, M. Nagase, K. Iwadate, and K Murase, “Dimensional limitations of silicon nanolines resulting from pattern distortion due to surface-tension of rinse water”, Appl. Phys. Lett. **66**: 2655–2657 (1995)

[Pokoy2009] B. Pokroy, S. H. Kang, L. Mahadevan, and J Aizenberg, “Self-Organization of a Mesoscale Bristle into Ordered, Hierarchical Helical Assemblies”, *Science* **323**: 237-240 (2009)

[Raccurt2004] O. Raccurt, F. Tardif, F. A. d‘Avitaya, and T. Vareine, “Influence of liquid surface tension on stiction of SOI MEMS“, J. Micromech. Microeng. **14**, 1083 (2004)

[Ruiz-Gutierrez2018] E. Ruiz-Gutiérrez, C. Semprebon, G. McHale., and R. Ledesma-Aguilar, “Statics and dynamics of liquid barrels in wedge geometries”, *Journal of Fluid Mechanics* **842**: 26-57 (2018)

[Roman2010] B. Roman and J. Bico, “Elasto-capillarity: deforming an elastic structure with a liquid droplet”, *J. Phys.: Condens. Matter* **22**: 493101 (2010)

[Shin2018] D. Shin and S. Tawfick, „Polymorphic Elastocapillarity: Kinetically Reconfigurable Self-Assembly of Hair Bundles by Varying the Drain Rate“, Langmuir **34**: 6231- 6236 (2018)

[Singh2014] K. Singh, J. R. Lister, and D. Vella, “A fluid-mechanical model of elasto-capillary coalescence”, *J. Fluid Mech.* **745**: 621-646 (2014)

[Taffetani2015] M. Taffetani and P. Ciarletta, “Elastocapillarity can control the formation and the morphology of beads-on-string structures in solid fibers”, *Physical Review E* **91**: 032413 (2015)

[Taroni2012] M. Taroni and D. Vella, “Multiple equilibria in a simple elastocapillary system”, *J. Fluid Mech.* **712**, 273 (2012)

[Wei2014] Z. Wei and L. Mahadevan, “Continuum dynamics of elastocapillary coalescence and arrest”, *EPL* **106**: 14002 (2014)

[Wei2015] Z. Wei, T. M. Schneider, J. Kim J, H-Y Kim, J. Aizenberg, and L. Mahadevan Elastocapillary coalescence of plates and pillars. *Proc. R. Soc. A* **471**: 20140593 (2015)

[Yang2009] Yang and G. Homsy, “Capillary instabilities of liquid films inside a wedge”, *Physics of Fluids* **19**: 044101 (2007)

4 Requested modules/funds

4.1 Basic Module

4.1.1 Funding for Staff

One PhD position according to the salary grade ¾ of TVL (E 13) including an overhead corresponding to 22% of the total budget

4.1.2 Direct Project Costs

None

4.1.2.1 Equipment up to Euro 10,000, Software and Consumables

Sample fabrication of masters by photolithograpy requies photomasks, photoresits, and solvents which amounts to costs of 2700 € p.a.

4.1.2.2 Travel Expenses

Participation of the PhD student in a national conference (5 days 1 person): 900 € and international conference (each 5 days 1 person): 2000 €

4.1.2.3 Visiting Researchers (excluding Mercator Fellows)

n.a.

4.1.2.4 Expenses for Laboratory Animals

n.a.

4.1.2.5 Other Costs

n.a.

4.1.2.6 Project-related publication expenses

Usuall allowance of 750 € publication fees p.a.

4.1.3 Instrumentation

4.1.3.1 Equipment exceeding Euro 10,000

n.a.

4.1.3.2 Major Instrumentation exceeding Euro 50,000

n.a.

4.2 Module Temporary Position for Principle Investigator

n.a.

4.3 Module Replacement Funding

n.a.

4.4 Module Temporary Clinician Substitute

n.a.

4.5 Module Mercator Fellows

n.a.

4.6 Module Workshop Funding

n.a.

4.7 Module Public Relations Funding

n.a

5 Project requirements

5.1 Employment status information

Dr. rer. Nat. Martin Brinkmann is a researcher at the Saarland University and works in the group of Prof. Dr. Ralf Seemann on a non-permanent contract until the end of January 2021. A prolongation of the contract until the end of the funding period is intended.

5.2 First-time proposal data

n.a.

5.3 Composition of the project group

Dr. Martin Brinkmann will supervise the project at the Saarland University.

5.4 Cooperation with other researchers

To foster the exchange between theoretical groups working with continuum-theoretical approaches within the SPP, we have initiated an informal network, which includes the groups of M. Brinkmann, S. Gurevich, D. Peschka, J. Snoeijer, H. Stark, U. Thiele, A. Voigt, and B. Wagner, and which is open to others. There, we will coordinate aspects of the training of the involved young researchers within the SPP, and meet sporadically to discuss details of our approaches and ongoing work.

5.4.1 Researchers with whom you have agreed to cooperate on this project

5.4.2 Researchers with whom you have collaborated scientifically within the past three years

- Dr. Ciro Semprebon, Northumbria University, Newcastle, UK
- Prof. Giampaolo Mistura, University of Padova, Padova, Italy
- Prof. Lou Kondic, New Jersey Institute for Science and Technology
- Prof. Stephan Herminghaus, Max-Planck Institute for Dynamics and Self-Organization, Göttingen

5.5 Scientific equipment

n.a.

5.6 Project-relevant cooperation with commercial enterprises

n.a.

5.7 Project-relevant participation in commercial enterprises

n.a.

6 Additional information

n.a.